2017

Valveless pumping: the reflected pulse wave hypothesis

Charles F. Babbs
Purdue University, babbs@purdue.edu

Valveless pumping: the reflected pulse wave hypothesis

Charles F. Babbs, MD, PhD

Weldon School of Biomedical Engineering, Purdue University,

West Lafayette, Indiana 47907, USA

Abstract

Valveless pumping refers to nonzero mean flow of fluid within a closed loop of viscoelastic tubing, when a compliant section of the loop is rhythmically compressed at particular frequencies. Valveless pumping is thought to play a role in blood circulation in embryos and in cardiopulmonary resuscitation (CPR). Heretofore, the physical mechanism causing valveless pumping has remained a mystery.

We consider closed loops composed of one length of soft, compliant tubing and one length of stiff, non-compliant tubing having equal internal diameters. The loops are filled with water and are compressed toward one end of the soft section. To model such pumps we characterize pulse (pressure) waves in the soft section using the classical wave equation assuming complete reflection of the pulse waves at the soft/stiff boundaries. Pulse wave velocity is specified by the Moens-Korteweg equation. The resulting instantaneous pressure difference across the fluid in the stiff segment is computed, and Newton's second law is used to describe the instantaneous and time averaged movement of fluid through the stiff segment and around the loop.

Mean flow equals zero if compression is performed at the midpoint of the soft segment. However, when changes in pulse wave velocity caused by expansion of the uncompressed regions of the soft segment are properly accounted for, nonzero mean flow develops during asymmetrical compression of the soft segment. The magnitude and direction of mean flow depend upon the compression frequency and can be reversed simply by changing from one compression frequency to another. Other parameters, such as compression point location and stiffness constants also act to determine the magnitude and direction of flow. Reflected pulse waves explain the existence and major features of valveless pumping on the basis of classical Newtonian physics.

I. INTRODUCTION

Imagine a closed loop of flexible rubber tubing filled with water or a similar incompressible fluid. The loop is about 30 cm in circumference, and the tubing is about 1 cm in diameter. Now imagine yourself squeezing a short segment of the loop between your thumb and forefinger about once each second (Figure 1). Can you predict the motion of the fluid in the loop?

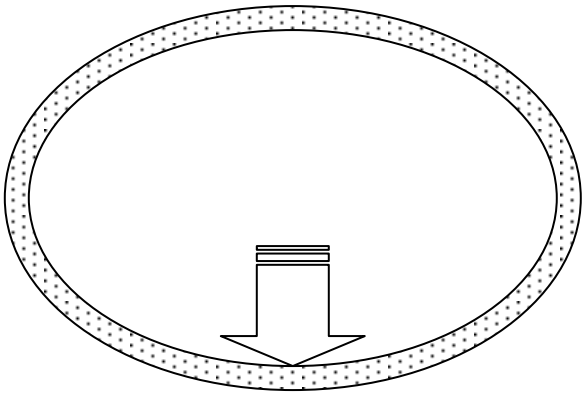

Figure 1. A thought experiment. Rhythmic compression of a fluid-filled elastic tube.

Most persons would probably predict that as the tubing is compressed a small amount of fluid would flow away from the compression point in both directions equally, distending the remainder of the loop slightly. Then, when compression is released, fluid would flow back again with no net flow in either direction around the loop. This intuitive prediction is correct for some cases. However, several previous reports have described such systems in which there is indeed a net flow of fluid in either the counterclockwise or clockwise direction[1-3]. This phenomenon is called "valveless pumping", because unidirectional net flow can occur in a closed circulatory system without valves. Such pumps can be made very inexpensively for the purpose of classroom demonstration.

Flow in valveless pumps is not steady but rather fluctuates. At certain frequencies there is a nonzero mean flow, which typically may be clockwise at one frequency and counterclockwise at another. A key required condition, slyly not indicated in Figure 1, is that the stiffness of the tubing is not uniform around the loop. The stiffness must vary in different segments of the loop for valveless pumping to occur, as shown in Figure 2. Here the loop includes only two segments, a stiff segment and a complaint segment having equal internal diameters. If the compliant segment is compressed at its exact midpoint, no net flow occurs. However, if the compliant segment is compressed asymmetrically at a point, L_c, non-zero average flow in one direction or the other can

develop at certain frequencies[2]. Indeed flow can be reversed in the loop, simply by changing frequencies—all without valves.

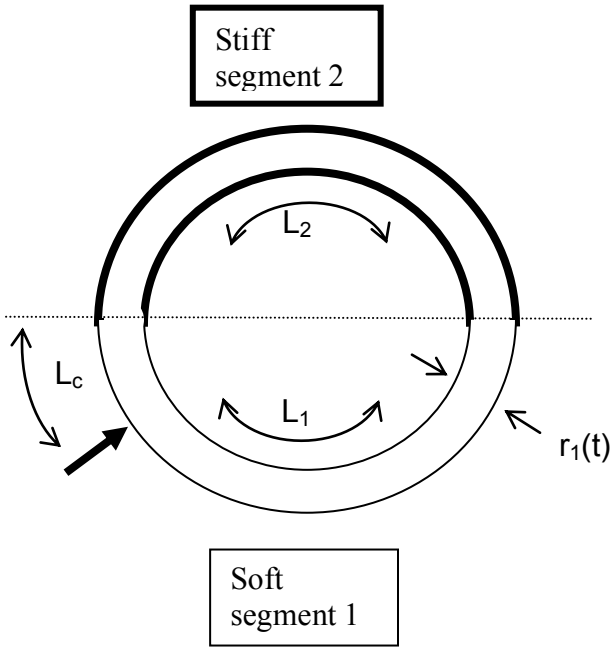

Figure 2. More detailed diagram of a valveless pump. Bold arrow indicates the point of rhythmic compression.

Valveless pumps may be more than laboratory curiosities. In developing embryos it is known that the heart develops and blood circulates before the development of functional heart valves[3, 4]. Perhaps at these early times the embryonic heart is acting as a valveless pump. In some models of cardiopulmonary resuscitation (CPR) artificial circulation of blood may occur when at least some of the cardiac valves are not functioning[5, 6], leading us to speculate that valveless pumping may be one of the mechanisms of blood flow during the external chest compressions of CPR. If valveless pumping occurs at very small physical scales, valveless pumps might be easily fabricated for micro machines, owing to their simple geometry and requirement for only a single moving part to provide external compression. A piezo crystal, which deforms in response to an applied voltage[7], might be used to power such a miniature pump.

To date the physical mechanism underlying valveless pumping, especially flow reversal at different frequencies, has remained a mystery[2]. Finding an explanation for the unidirectional mean flow is a challenging problem. One of us[2] has described a partial differential equation (PDE) model of a valveless pump using the immersed boundary method. This system is capable of predicting the essential features of valveless pumping in two dimensions. However, the complexity of the system of equations does not provide a satisfying intuitive explanation for why valveless pumping occurs.

One useful outgrowth of the immersed boundary work was the production of an animation showing details of flow around the loop, which may be viewed on the Internet[8]. This animation of a valveless pump of the type shown in Figure 2 suggests that as external compression occurs, pulse waves are generated and travel along the walls of flexible segment 1. For the usual case when stiff segment 2 is almost rigid (substantially stiffer than segment 1) it is clear that the pulse waves are reflected at the compliant-stiff boundary and travel back and forth in the compliant segment. Further, fluid flow in the stiff segment is relatively steady and laminar[2], while flow in the flexible segment is faster, bidirectional, and complex.

These observations led to the pulse wave reflection hypothesis, namely that valveless pumping happens because pulse waves are reflected between the ends of the compliant segment and in so doing create interference patterns that can generate pressure differences across the ends of the stiff segment, which can support nonzero mean flow. For simplicity, we assume that the stiff segment is infinitely stiff and that the radius to length ratio of the soft segment is small, so that wave propagation becomes one-dimensional. If true, the pulse wave reflection hypothesis would provide a relatively simple explantation of valveless pumping based upon classical Newtonian physics.

Accordingly, the objective of the present research was to develop a mathematical formulation of the pulse wave reflection hypothesis that demonstrates the phenomena of valveless pumping and reveals the physical principles that govern flow. Aspects of the requisite analysis include descriptions of pulse waves in an elastic tube, pulse wave velocity and reflection, the pressure difference between the ends of the stiff segment, the governing equation for motion of fluid in the stiff segment, and numerical results.

II. THEORY

A. Overview

According to the reflected pulse wave hypothesis, pulse waves from the external driving compressions are largely reflected at the ends of the compliant segment of the loop. Most of the wave energy, rather than circumnavigating the loop, bounces back and forth along the compliant segment, becoming gradually attenuated by viscous forces. The reflected waves add in phase or out of phase with more recent pulses depending on the specific driving frequency and the geometry and physical properties of the soft segment. In turn, the net pressure on the two ends of the column of fluid in the stiff segment induces its motion. The mass of the fluid in the soft segment is entrained with that in the stiff segment and pulled along with it in the circuit.

If the various incident and reflected waves were always sinusoidal in the time domain, then the mean pressure at each end of compliant segment 1 would always be zero, because the mean value of any whole number of sinusoidal waves in any phase is zero. However, because the average radius of compliant segment 1 changes with external compression (it becomes larger along most of its length), pulse wave velocity changes during the compression cycle, generating somewhat non-sinusoidal waves. According to the reflected pulse wave hypothesis, the resulting waveform distortions can produce a net driving pressure causing preferential flow in one direction. As will be shown, the required waveform distortions can be understood in terms of changing pulse propagation times from the compression point to the two ends of the soft segment. These fluctuating delays are caused by distension related changes in pulse wave velocity. Definitions of variables used in the following discussion are provided in Table 1.

Table 1. Nomenclature.

Symbol	Definition	Units
Known variables		
A	Internal cross-sectional area of stiff segment	cm^2
f	Frequency of external pumping	Hz
r (0)	Initial internal radius of soft and stiff segments	cm
$r_1(t)$	Time varying internal radius of soft segment	cm
L_1, L_2	Axial lengths of soft and stiff segments	cm
Lc	Distance from compression point to left hand end of soft segment	cm
$h_1(t)$, h_2	Thicknesses of soft and stiff segments	cm
E_1, E_2	Elastic (Young's) moduli of wall materials of soft and stiff segments	$dynes/cm^2$
ρ	Density of fluid inside valveless pump	g/cm^3
SV	Stroke volume of compression	cm^3
β	Wave attenuation factor	cm^{-1}
ν	Viscosity of fluid inside valveless pump	g/cm/sec
Derived variables		
ω	Angular frequency of external pumping	Hz
C_1, C_2	Compliances of soft and stiff segments	$cm^5/dyne$
R_1, R_2	Resistances of soft and stiff segments	$cm^5/dyne$
R_{tot}	Total resistance of soft and stiff segments	$cm^5/dyne$
L_{tot}	Total axial length of soft and stiff segments	cm
s(t)	Pulse wave velocity in soft segment	cm/sec
$\bar{s}(\tau, t)$	Average pulse wave velocity during the last τ seconds	cm/sec
Δx_E	Distance from compression point to right hand end of soft segment ($=L_1 - L_c$)	cm
Δx_W	Distance from compression point to left hand end of soft segment ($= L_c$)	cm
y(t)	Instantaneous flow in segment 2	cm^3
λ	Pulse wavelength in soft segment 1, $\lambda = s/f$	cm

B. Pressure waves in elastic tubes

Pressure waves travel in thin walled, distensible tubes propagate at a particular speed (the so-called pulse wave velocity) classically described by the Moens-Korteweg equation[8]

$$s(t) = \sqrt{\frac{E\,h(t)}{2\rho\,r(t)}}\ , \qquad (1)$$

where $h(t)$ is the wall thickness of a tube of radius, $r(t)$, at time t. The tube is composed of material having Young's modulus of elasticity, E, and filled with fluid of density, ρ.

In addressing the problem of valveless pumping, we are concerned with distensible tubes, for which increases in the radius lead to decreases in wall thickness. For such tubes by geometry (assuming conservation of wall volume, i.e. Poisson's ratio = 0.5, and a thin wall $h(0) << r(0)$), then $2\pi r(0)h(0) \cong 2\pi r(t)h(t)$ for any time, t, or

$$\frac{h(t)}{r(t)} \cong \frac{r(0)h(0)}{r^2(t)}\ . \qquad (2)$$

Thus the Moens-Korteweg equation for thin walled, stretched tubes can be re-written as

$$s(t) = \sqrt{\frac{Eh(t)}{2\rho r(t)}} \cong \sqrt{\frac{E\,r(0)\,h(0)}{2\rho}} \cdot \frac{1}{r(t)} = s(0) \cdot \frac{r(0)}{r(t)} \qquad (3)$$

When the soft segment is squeezed at the compression point, fluid is moved into the uncompressed portion of the soft segment and increases its radius. As $r(t)$ increases, pulse wave speed, $s(t)$, decreases and pulse wave propagation slows. This relationship is critically important to the problem of valveless pumping.

C. Instantaneous pulse wave velocity in a soft tube with changing volume, V(t)

Suppose a thin walled elastic tube of radius, r, and axial length, L, is injected with a small volume dV(t) to produce pulses that travel along the tube. As shown in Figure 3, the effect is similar to external compression but is easier to analyze. For sinusoidal changes, the volume of the tube may be written as

$$V(t) = V(0) + dV(t) = V(0) + \frac{1}{2} SV(1 - \cos(\omega t)), \qquad (4)$$

where $V(0) = \pi r^2(0) L$ is the initial volume inside compliant segment 1 having initial radius, r(0), and the angular frequency and stroke volume for external compression are ω and SV, respectively.

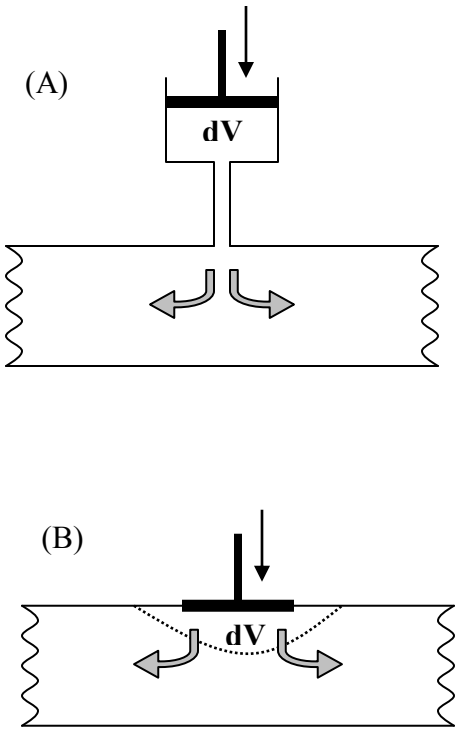

Figure 3. Equivalence of injection of a small volume (A) with a small external compression (B). Both maneuvers expand the radius of the soft segment away from the compression site to cause small changes in pulse wave velocity. Only a short section near the compression point is shown.

In the problem of valveless pumping, if a small region of the tube is compressed externally, the volume dV(t) swept out by the compression is injected into the remaining parts of the tube (Figure 3(B)). The total volume within the loop is unchanged. However there is a change in volume of the uncompressed regions as if dV(t) were injected at the point of compression. Note that the volume of the compressed segment is small with respect to the total volume within segments 1 and 2. Thus when reflected pulses later return to the compression point, they traverse the compression zone without being substantially changed. That is, the differences in pulse transit times through the compression zone are small, because its length is small with respect to the rest of segment 1.

Now consider a fixed length elastic tube, the volume of which is $V(t) = \pi r^2(t) L$. Using our standard nomenclature, the pulse wave velocity along the tube is given by Eq. (3), as

$$s(t) \cong s(0) \cdot \frac{r(0)}{r(t)} = s(0) \sqrt{\frac{V(0)}{V(t)}} . \tag{5}$$

From Eq. (4)

$$\frac{V(t)}{V(0)} = 1 + \frac{1}{2} \frac{SV}{V(0)} (1 - \cos(\omega t)) . \tag{6}$$

Hence,

$$s(t) \cong s(0) \left(1 + \frac{1}{2} \frac{SV}{V(0)} (1 - \cos(\omega t)) \right)^{-\frac{1}{2}} \tag{7}$$

For smaller stroke volumes $SV/(2\ V(0)) << 1$, and using the Taylor's series expansion

$(1 + x)^{-\frac{1}{2}} \cong 1 - \frac{1}{2} x$, for $x << 1$ we have

$$s(t) \cong s(0) \left(1 - \frac{1}{4} \frac{SV}{V(0)} (1 - \cos(\omega t)) \right) . \tag{8}$$

Thus the instantaneous pulse wave speed in the soft segment at any time t is

$$s(t) \cong s(0) \left[1 - \varepsilon (1 - \cos(\omega t)) \right] = s(0)(1 - \varepsilon) + s(0) \cdot \varepsilon \cdot \cos(\omega t) , \tag{9}$$

where $\varepsilon = \frac{1}{4} \frac{SV}{V(0)}$.

The pulse wave velocity, s(t), shows small sinusoidal fluctuations about its mean value, s(0)(1-ε).

From Eq. (9) we can find the average pulse wave speed, $\bar{s}$, and transit time, τ, for a pulse wave traveling over a certain fixed distance, Δx, from the compression point during a certain epoch of time. These values are important in order to determine the net pressure at the opposite ends of segment 2 from various reflected waves. As the effective soft segment volume, V(t), changes sinusoidally with time, pulse wave velocity, s(t), varies also, as expected from the Moens-Korteweg equation. It is the average pulse wave velocities, and attendant propagation delays, over various intervals, Δx, that are critical to the mechanism of valveless pumping.

D. Average pulse wave velocity, $\bar{s}$, and transit time, τ

The mean value of s(t) over the interval t_1 to t_2 is

$$\bar{s}(t_1, t_2) = \frac{1}{t_2 - t_1}\int_{t_1}^{t_2} s(t)dt\,. \tag{10}$$

Substituting for s(t),

$$\bar{s}(t_1, t_2) = \frac{s(0)(1-\varepsilon)}{t_2 - t_1}\int_{t_1}^{t_2} dt + \frac{s(0)\varepsilon}{t_2 - t_1}\int_{t_1}^{t_2} \cos(\omega t)dt$$

$$= s(0)(1-\varepsilon) + \frac{s(0)\varepsilon}{t_2 - t_1}\left(\frac{1}{\omega}\sin(\omega t)\right]_{t_1}^{t_2}$$

$$= s(0)(1-\varepsilon) + \frac{s(0)\varepsilon}{(t_2 - t_1)\omega}\left(\sin(\omega t_2) - \sin(\omega t_1)\right). \tag{11}$$

If $t_2 = t$ and $t_1 = t - \tau$, then the average wave speed during the last τ seconds of pulses traveling in segment 1 is

$$\bar{s}(\tau, t) = s(0)(1-\varepsilon) + \frac{s(0)\varepsilon}{\tau\omega}\left(\sin(\omega t) - \sin(\omega(t-\tau))\right). \tag{12}$$

Suppose pulse transit time $\tau(\Delta x, t) = \dfrac{\Delta x}{\bar{s}(\tau, t)}$ for some distance, Δx, just traveled by a pulse wave. Then,

$$\bar{s}(\tau,t) = \frac{\Delta x}{\tau(\Delta x,t)} = s(0)(1-\varepsilon) + \frac{s(0)\,\varepsilon}{\tau(\Delta x,t)\,\omega}\left(\sin(\omega t) - \sin(\omega(t-\tau(\Delta x,t))\right) \qquad (13)$$

is a nonlinear equation that can be solved for the transit time, $\tau(\Delta x,t)$, of a pulse wave previously arising distance, Δx, away. Pulse transit time will be needed in section G. to describe pressures in the soft segment of the valveless pump in terms of Eq. (20), which is the classical wave equation.

E. Reflection of pressure waves in elastic tubes at a stiffness boundary

If the ends of stiff segment 2 are essentially immobile, then as shown in Jung's movie[8, 9], pulse waves are reflected back and forth in the flexible segment 1 without inversion. Unlike pulse waves on a flexible string, which are reflected with inversion at a fixed end, here the reflection is similar to waves at the vertical edge of a swimming pool or fish tank. The mass of fluid in a wave peak builds up at the boundary and then falls back upon itself in the process of reflection. Pulse waves depart from the compression point, are reflected from the ends of the stiff segment, and return toward the compression point. The reflection coefficient is assumed to be +1.0, in agreement with the detailed analysis of Alderson and Zamir[10].

F. Governing differential equation for flow in stiff segment 2

In general, the reflected pulse wave hypothesis states that the net pressure difference between the ends of the fluid column in stiff segment 2 provides an asymmetrical driving pressure that causes forward or backward flow. In turn, Newton's second law of motion gives the motion of the fluid column in segment 2.

In Figure 4 the parallel lines represent the straightened stiff segment 2 of length, L_2. $P_E(t)$ and $P_W(t)$ are the pressures at opposite (East and West) ends joining the soft segment 1, which is not shown. Flow through segment 2 is denoted y(t) and is defined as positive for flow from $P_E(t)$ to $P_W(t)$. The classical resistance of segment 2 is a constant, R_2, with units of pressure divided by flow. The mean fluid velocity is $v(t) = y(t)/A$, where $A = \pi r(0)^2$ is the cross sectional area of the stiff segment.

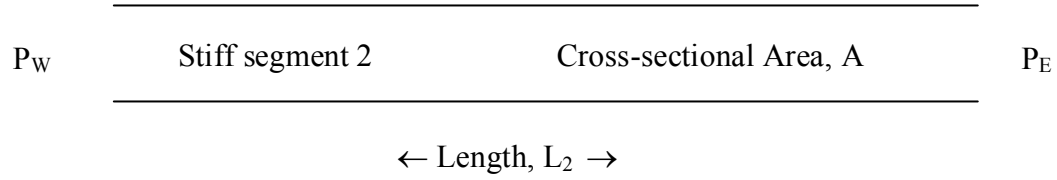

Figure 4. Straightened stiff segment 2.

The force overcoming the resistance to fluid flow in segment 2 (push + pull) is

$$F_R(t) = y(t)R_2 A. \tag{15}$$

The force overcoming the inertia of the fluid column in segment 2 by Newton's second law (Force = mass*acceleration) is

$$F_I(t) = \rho A L_2 \frac{dv(t)}{dt} = \rho L_2 \frac{dy(t)}{dt}. \tag{16}$$

Adding,

$$F_R(t) + F_I(t) = (P_E(t) - P_W(t))A = y(t)R_2 A + \rho L_2 \frac{dy(t)}{dt}. \tag{17}$$

If the fluid in segment 2 were disposed in a straight line and otherwise unconstrained, its motion would be given by

$$(P_E(t) - P_W(t)) = y(t)R_2 + \frac{\rho L_2}{A}\frac{dy(t)}{dt}. \tag{18}$$

However, the fluid in segment 2 also must drag the fluid in segment 1 through its resistance while overcoming its inertia. In this sense the fluid in segment 1 is entrained with that in segment 2. The conceptual model is that the fluid in segment 1 is connected by massless strings to the fluid in segment 2 and is pulled along with it. The electrical engineering analogy is that of a battery. Segment 1 acts as a battery, which can be modeled as an ideal voltage (pressure) source, connected in series with an internal resistance, and in this case inductance[11]. When the battery is connected to a load resistance, flow around the circuit depends upon the sum of the load resistance and a fixed internal resistance of the battery. The equivalent circuit model for the battery is useful for computing flow through the load resistance, despite complex internal processes

and internal architecture of the battery. Similarly, for a valveless pump circuit we can write

$$(P_E(t) - P_W(t)) = y(t)R_{tot} + \frac{\rho L_{tot}}{A}\frac{dy(t)}{dt} \ , \qquad (19a)$$

where

$$R_{tot} = R_1(t) + R_2 \cong R_1(0) + R_2 \quad \text{and} \quad \frac{\rho L_1}{A_1(t)} + \frac{\rho L_2}{A} \cong \frac{\rho L_{tot}}{A} \ . \qquad (19b)$$

Here we ignore fluctuations in the resistance and inertance of the soft segment caused by changes in its cross sectional area (a small signal model).

Eq. (19a) is an ordinary differential equation (ODE) that one can solve knowing the driving pressure difference, $(P_E(t) - P_W(t))$, between the ends of the stiff segment 2. The result is the flow, y(t), through the "load" of segment 2, which is of central interest in the problem of valveless pumping.

G. Expression for driving pressure

Let us represent the driving pressure across segment 2 as $P_E(t) - P_W(t)$, where $P_E(t)$ is the total pressure at the right hand (East) end of segment 1 and $P_W(t)$ is the total pressure at the left hand (West) end of segment 1. Thus, positive flow is defined as counterclockwise around the loop by analogy with a racetrack or a geometric angle.

Consider reflected pressure waves moving back and forth across soft segment 1 as shown in Figure 2, with reflections occurring alternately at its right hand (East) end, distance Δx_E from the compression point, and at its left hand (West) end, distance Δx_W from the compression point. (Note that in Figure 2 $\Delta x_E = L_1 - L_c$ and $\Delta x_W = L_c$.) Let $P_E^a(t)$ indicate the pressure at the right hand end of segment 1 due to pulse a, traveling initially from the compression point to the right. Let $P_E^b(t)$ indicate the pressure at the right hand end of segment 1 due to pulse b, traveling initially from the compression point to the left. The total pressure at the right hand end of segment 1 is $P_E(t) = P_E^a(t) + P_E^b(t)$. Similarly, the total pressure at the left hand end of segment 1 is $P_W(t) = P_W^a(t) + P_W^b(t)$.

Suppose that the pressure waves traversing segment 1 are described by the classical wave equation[12], such that the pressure distance Δx from the compression point at time, t, is

$$F(\Delta x, t) = P_{max} \sin\left(\omega(t - \tau(\Delta x, t)) - \phi\right) e^{-\beta \Delta x} \ , \qquad (20)$$

where $\tau(\Delta x, t)$ is the pulse propagation delay experienced by a pulse arriving at time, t, some distance, Δx, from the compression point. An exact expression for computing $\tau(\Delta x, t)$ was developed previously in section D. Angle ϕ is the phase angle between the driving flow and the pressure wave, if any. The damping constant, β, describes the viscoelastic decay of the pulse wave with distance[13].

Consider the pressure at the right hand end of segment 1, distance Δx_E from the compression point. Assume that all waves are completely reflected at the compliant/stiff boundary without inversion when the stiff segment is completely rigid (i.e. $E_2 \to \infty$)[10]. Then, accounting for the immediate reflection of each pulse wave[10, 14], by multiplying by a factor of 2,

$$P_E^a(t) = 2F(\Delta x_E, t) + 2F(\Delta x_E + 2L_1, t) + 2F(\Delta x_E + 4L_1, t) + 2F(\Delta x_E + 6L_1, t)\cdots$$
$$= \sum_{i=0}^{n} 2F(\Delta x_E + 2iL_1, t) \tag{21}$$

is the pressure at the east end of the soft segment from addition of n successive reflections of pulse wave a. When n becomes large, the n-th term becomes negligibly small because of the exponential decay in F.

The pressure at the East end from successive arrivals of pulse b, initially traveling to the left and reflected an odd number of times is

$$P_E^b(t) = 2F(\Delta x_W + L_1, t) + 2F(\Delta x_W + 3L_1, t) + 2F(\Delta x_W + 5L_1, t)\cdots$$
$$= \sum_{i=0}^{n} 2F(\Delta x_W + (2i+1)L_1, t) \tag{22}$$

Similarly,

$$P_W^a(t) = 2F(\Delta x_E + L_1, t) + 2F(\Delta x_E + 3L_1, t) + 2F(\Delta x_E + 5L_1, t)\cdots$$
$$= \sum_{i=0}^{n} 2F(\Delta x_E + (2i+1)L_1, t) \tag{23}$$

and

$$P_W^b(t) = 2F(\Delta x_W, t) + 2F(\Delta x_W + 2L_1, t) + 2F(\Delta x_W + 4L_1, t) + 2F(\Delta x_W + 6L_1, t)\cdots$$
$$= \sum_{i=0}^{n} 2F(\Delta x_W + 2iL_1, t) \tag{24}$$

Now, the driving pressure across stiff segment 2 can be computed numerically as

$$\Delta P(t) = P_E(t) - P_W(t) = P_E^a(t) + P_E^b(t) - P_W^a(t) - P_W^b(t)$$

$$= 2\left[F(\Delta x_E, t) - F(\Delta x_E + L_1, t) + F(\Delta x_E + 2L_1, t) - F(\Delta x_E + 3L_1, t) + \cdots\right]$$

$$- 2\left[F(\Delta x_W, t) - F(\Delta x_W + L_1, t) + F(\Delta x_W + 2L_1, t) - F(\Delta x_W + 3L_1, t) + \cdots\right]. \quad (25)$$

This driving pressure, $\Delta P(t)$, is readily computed from the given constants and the initial conditions describing a particular valveless pump.

H. Specification of P_{max}

There remains the issue of specifying the constant P_{max} in the wave equation $F(\Delta x, t)$. One approach is to consider P_{max} as another given constant. However, practical valveless pumps tend to be specified, not in terms of the applied pressure, but in terms of the length and distance of external compression of segment 1, creating a stroke volume, SV. One approach to relating P_{max} to SV and other known variables in Table 1 is shown in Figure 5.

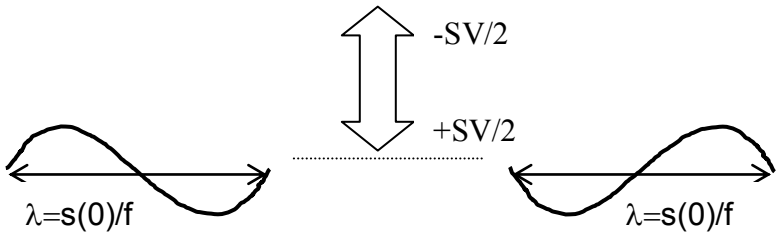

Figure 5: Sketch of pulse waves departing from compression point in both directions.

Imagine an infinitely long soft tube having properties like segment 1 and compressed at its midpoint a volume ± one half SV in a sinusoidal fashion. Assume that the viscous forces in the wall are small, so that the changes in local radius are directly proportional to the change in local pressure, as is typical for thin walled tubes. A traveling wave will propagate away from the compression point in each direction. Considering the traveling waves in space, there are segments of the tube that are alternately expanded and contracted by a volume one quarter SV (since one half of one half SV is injected in each direction). Thus sinusoidal compression will create a pattern of bulges and constrictions in the tube along its length. Each outward bulge is one half wavelength, λ, long, where $f\lambda \cong s(0)$, for compression frequency, f. (Wavelength, λ, actually fluctuates slightly, because s(t) fluctuates slightly; but for the purpose of estimating P_{max} we can ignore this small change.) Each inward constriction is also about one half wavelength, λ , long.

Thus a sinusoidal variation in volume, distributed along one wavelength, propagates as a wave away from the compression point in each direction.

The mean pressure in the half wavelength segment is given approximately by the ratio of injected volume to compliance or

$$\overline{\Delta P} = \frac{\frac{1}{4}SV}{C(\frac{1}{2}\lambda)}, \tag{26}$$

where

$$C(x) = \frac{2\pi x r^3(0)}{Eh(0)} \tag{27}$$

is the compliance of an x-length segment of the tube.

Now suppose further that the pressure wave shape is sinusoidal, the ratio of the peak to mean value for the quarter wavelength sinusoidal wave is $\pi/2$. Substituting $x = \frac{1}{2}\frac{s(0)}{f}$,

$$P_{max} = \frac{\frac{\pi}{2}\cdot\frac{1}{4}\cdot SV}{\frac{2\pi\left(\frac{1}{2}\frac{s(0)}{f}\right)r^3(0)}{Eh(0)}} = \frac{1}{8}\cdot\frac{SV\cdot Eh(0)f}{s(0)\,r^3(0)}. \tag{28}$$

Note P_{max} is an increasing linear function of the frequency when the SV and other parameters are fixed.

III. NUMERICAL METHODS

Computer programs were developed independently by each co-author for solving Eq. (19). Results of the two programs for instantaneous flow in the valveless pump were checked against each other.

A. Specifications

In a typical valveless pump of the type shown in Figure 2, a compliant segment of length L_1 is connected in series with a stiff walled segment of length L_2. The initial inner radius of each segment is r(0), and the segments are connected so that there is no discontinuity in diameter at the junctions between the soft and stiff segments. At the arrow, the left

hand portion of compliant segment 1 is compressed externally at a sinusoidal frequency, f. The stroke volume of external compression is SV. External compression is applied at a circumferential distance L_c from the left hand boundary between the two segments. Other relevant parameters are defined in Table 1. Typical values for a test case, similar to those described by Jung, are shown in Table 2.

Table 2. Particular parameters specifying a standard valveless pump.

Parameter and symbol	**Value**	**Units**
Segment length, L_1	10	cm
Segment length, L_2	20	cm
Initial internal radius, $r(0) << L_1$	0.5	cm
Wall thicknesses h_1 and h_2	0.1	cm
Elastic modulus, E_1	1000	$g/cm/sec^2$
Elastic modulus, E_2	Infinite	$g/cm/sec^2$
Water density, ρ	1.0	g/cm^3
Water viscosity, ν	0.01	g/cm/sec
Drive stroke volume, SV	1.0	cm^3

The resistance of each segment of the valveless pump was given by Poiseuille's law[15]:

$$R_i = \frac{8 L_i \nu}{\pi r_i(0)^4} \quad \text{for i = 1 (soft boundary) or i = 2 (stiff boundary),} \tag{29}$$

where ν is the viscosity of the fluid in the tube. The compliance of each segment is readily derived from calculus[16] and is given by

$$C_i = \frac{2\pi L_i r_i(0)^3}{E_i h_i(0)} \quad \text{for i = 1 (soft wall) or i = 2 (stiff wall).} \tag{30}$$

B. Solving for mean pulse delay time, $\tau(\Delta x, t)$

Equation (13) can be solved recursively in the form

$$\tau(\Delta x, t) = \frac{\Delta x - \frac{s(0)\varepsilon}{\omega}\left(\sin(\omega t) - \sin(\omega(t - \tau(\Delta x, t))\right)}{s(0)(1-\varepsilon)} \tag{31}$$

with an initial guess of $\tau_1(\Delta x, t) = \frac{\Delta x}{s(0)(1-\varepsilon)}$.

Because ε is small (i.e. stroke volume is small with respect to the total volume of segment 1), $\tau_1(x,t)$ is a good initial guess, easily refined by the iterative process.

C. Solving for flow y(t)

Thus, the governing differential equation for flow in segment 2 is

$$y(t)R_{tot} + \frac{\rho L_{tot}}{A}\frac{dy(t)}{dt} = \Delta P(t)\,. \tag{32}$$

This is a first order differential equation of the form $\dot{y} = by + D(t)$

for constant $b = -\frac{AR_{tot}}{\rho L_{tot}}$ and function $D(t) = \frac{A}{\rho L_{tot}}\Delta P(t)$.

An exact solution for times $t \geq 0$ is given by

$$y(t) = \left[\int_0^t D(\xi)e^{-b\xi}\,d\xi + c\right]e^{bt} \tag{33a}$$

for constant, c. In our case y(0) = 0, so c = 0, and

$$y(t) = \left[\int_0^t D(\xi)e^{-b\xi}\,d\xi\right]e^{bt}\,. \tag{33b}$$

Beginning with initial conditions at t = 0, we found y(t) for various valveless pumps described in the results using numerical integration for $\left[\int_0^t D(\xi)e^{-b\xi}\,d\xi\right]$. The time step for numerical integration was typically 0.02/f seconds for frequency, f, making for 50 time steps per compression cycle. This approach provided fast and accurate numerical solutions for flow in segment 2 as a function of time.

IV. RESULTS

Figure 6 shows a complete frequency spectrum for the range 0.3 to 5 Hz. Here mean flow in periodic steady state for compressions 95-105 is plotted at each frequency. The compression point location was at $L_c = 2.5$ cm. The curve in Figure 6 represents flow in the standard model (Table 2) as described in Methods. For this model the radius of the uncompressed sections of compliant segment 1 expands as fluid is displaced from the much shorter compressed section. As a result, pulse wave velocity, s, in segment 1 decreases slightly as specified by the Moens-Korteweg equation. Under these

circumstances valveless pumping occurs at particular frequencies shown in Figure 6. In the range of 0.3 to 5 Hz maximums and minimums occur in a complex pattern. These results demonstrate the existence of valveless pumping, strong frequency dependence of the phenomenon, and reversal of flow with changes in frequency alone.

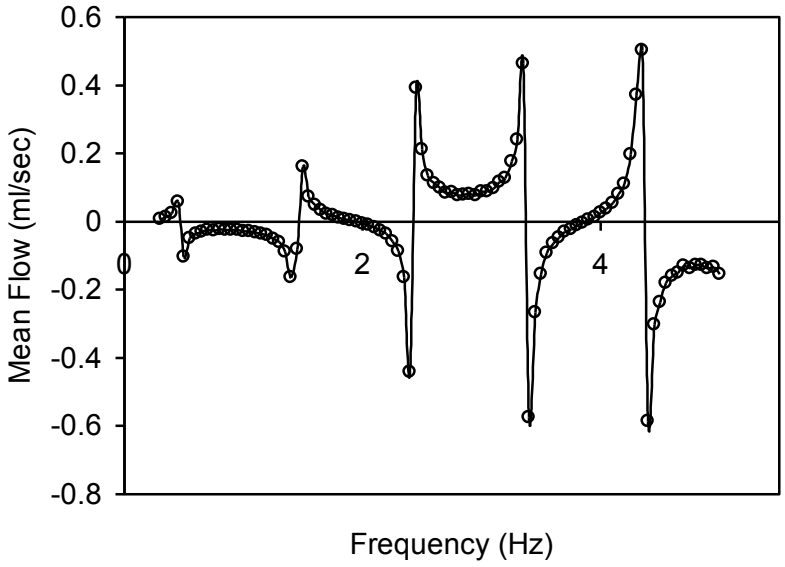

Figure 6. Frequency spectrum of mean flow in a valveless pump. Standard valveless pump model: Segment 1 length 10 cm, diameter 1 cm, wall thickness, 0.1 cm, Young's modulus 1000 dynes/cm^2, stroke volume 1 ml. Segment 2 length 20 cm, diameter 1 cm, wall thickness 0.1 cm, Young's modulus infinite. Damping constant beta = 0.01. Compression point location is halfway between the midpoint of L_1 and the left hand end of segment 1 (L_C = 2.5 cm). The time step for numerical integration was 0.02/frequency. Identical results to 3 significant figures were obtained when dt was halved to 0.01/frequency.

If pulse wave velocity in the soft segment is forced to be constant, that is s(t) is set equal to s(0) for all times, t, and all other conditions of the simulation are the same as before, then mean flow becomes zero for all frequencies tested. That is, valveless pumping does not occur unless pulse wave velocity varies properly as a function of segment 1 radius.

Results on the vertical axis of Figure 7 are plotted in terms of pump efficiency, defined as mean flow around the loop, divided by the product of frequency and stroke volume. The later product represents flow in a similar pump with properly functioning input and output valves, forcing unidirectional flow. In Figure 7 otherwise identical simulations are performed with stroke volumes decreasing from 1 to 0.25 ml. Pump efficiency decreases as stroke volume decreases and appears to extrapolate to zero as stroke volume approaches zero. Since pulsatile changes in radius of the flexible segment are directly

related to stroke volume, these results support the concept that radius related changes in pulse wave velocity are critical in sustaining nonzero mean flow around the loop.

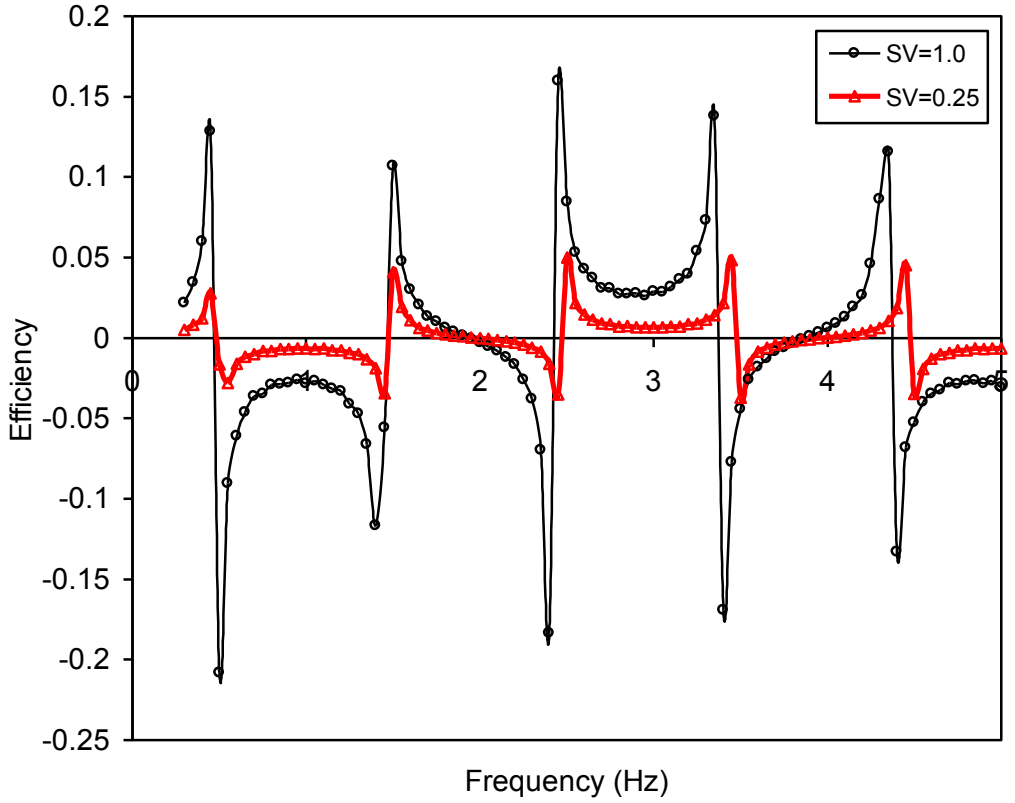

Figure 7. Pump efficiencies with varying stroke volume. Other details similar to Figure 6.

Instantaneous flow vs. time in a typical valveless pump of the type shown in Figure 2 is plotted in Figure 8 in the neighborhood of the 100th compression cycle after the achievement of periodic steady state. The two compression frequencies depict near maximal negative or clockwise flow (a) and near maximal positive or counterclockwise flow (b) from Figure 6. Only a very small change in frequency is needed to shift between these two states.

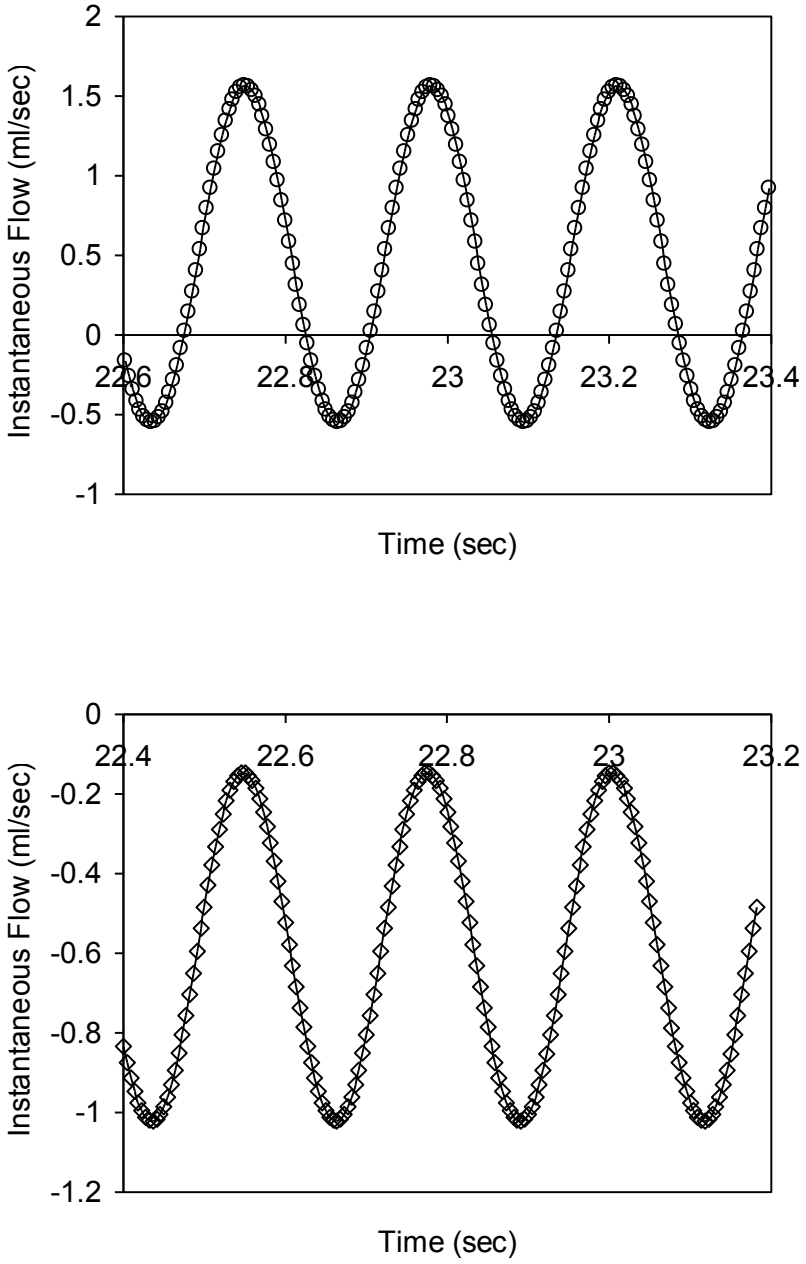

Figure 8. Time domain plots of instantaneous flow in a valveless pump reaching periodic steady state. Top curve: frequency = 4.35 Hz near a positive flow maximum in the frequency domain. Bottom curve: frequency = 4.40 Hz near a negative flow maximum. Flow reversal can occur with a small change in frequency. Standard valveless pump model: Segment 1 length 10 cm, diameter 1 cm, wall thickness, 0.1 cm, Young's modulus 1000 dynes/cm^2, stroke volume 1 ml, Segment 2 length 20 cm, diameter 1 cm, wall thickness 0.1 cm, Young's modulus infinite. Beta 0.01.

Figure 9 illustrates mean flow as a function of the location of the compression point in segment 1. As expected, zero flow in segment 2 occurs when the compression point is located at the exact midpoint of segment 1. An unexpected but logical result is that flow varies as a sinusoidal function of the distance from the midpoint of segment 1. The spatial wavelength of this sinusoidal function is $\lambda \cong s(0)/f$. Also, as expected from symmetry, compression to the right of the midpoint of segment 1 produces mean flow that is reversed in direction, compared with that caused by compression an equal distance to the left of the midpoint.

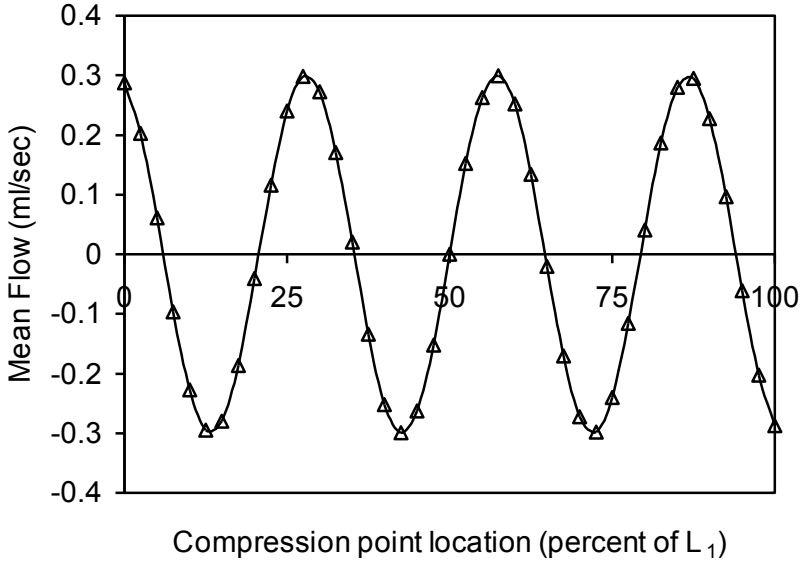

Figure 9. Flow in a standard model of a valveless pump as a function of compression point location. Compression frequency is 3.30 Hz. Standard valveless pump model: Segment 1 length 10 cm, diameter 1 cm, wall thickness, 0.1 cm, Young's modulus 1000 dynes/cm^2, stroke volume 1 ml. Segment 2 length 20 cm, diameter 1 cm, wall thickness 0.1 cm, Young's modulus infinite. Beta 0.01. Here wavelength $\lambda \cong s/f = \sqrt{(Eh)/(2\rho r)}/f = 10/3.3 = 3.0$ cm.

An exhaustive description of all parameter effects in the pulse wave reflection model is beyond the scope of this paper, however, one important class of effects should be mentioned. Changes in factors that affect baseline pulse wave velocity, s(0), produce characteristic shifts in the peaks of the frequency spectrum toward higher or lower frequency values. One important such factor is wall stiffness, or the product of wall stiffness and wall thickness. As illustrated in Figure 10, peak frequency shifts with stiffness and wall thickness of segment 1 according to the expression

$$\frac{f_2}{f_1} = \sqrt{\frac{E_2 h_2}{E_1 h_1}}\,. \qquad (34)$$

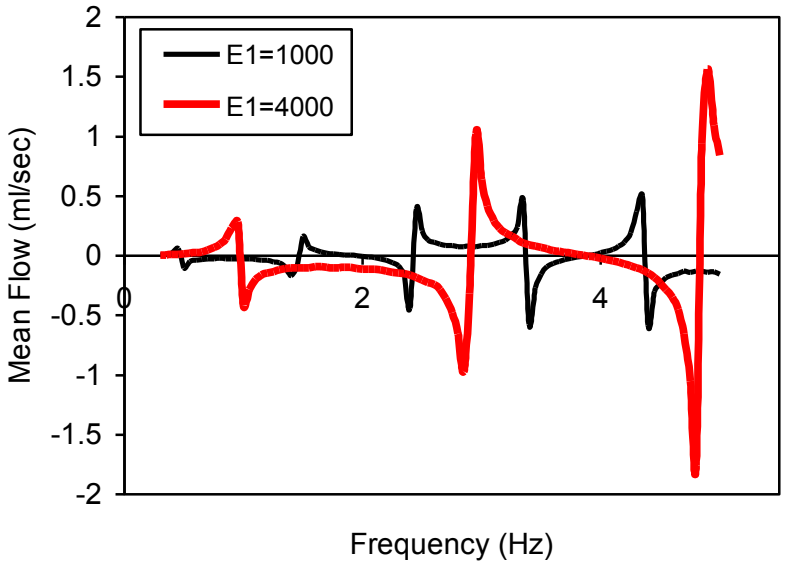

Figure 10. Peak frequency shifts with stiffness and wall thickness. $\frac{f_2}{f_1} = \sqrt{\frac{E_2 h_2}{E_1 h_1}}$. Amplitude of flow increases in proportion to stiffness and wall thickness. Other details similar to Figure 6.

Substituting a stiffer segment 1 shifts peaks in the flow spectrum to the right, toward higher frequencies. Substituting a softer segment 1 shifts peaks in the flow spectrum to the left, toward lower frequencies. Eq. 34 summarizes numerous computational examples and is based upon the concept that a given pressure difference across the end of the soft segment will occur when the east end of the soft segment is a particular number of wavelengths from the compression point and when the west end of the soft segment is another particular number of wavelengths from the compression point. Combinations of frequency and other parameters that give the same wavelength will have the same pressure difference and mean flow for the same stroke volume. Recognizing that impulse wavelength equals pulse wave velocity divided by frequency, $\lambda = s/f$, then

$$\frac{s_1}{f_1} = \frac{s_2}{f_2} \Rightarrow \frac{f_2}{f_1} = \frac{s_2}{s_1} = \frac{\sqrt{E_2 h_2}}{\sqrt{E_1 h_1}}. \qquad (35)$$

V. DISCUSSION

The phenomenon of valveless pumping is counterintuitive but real. The present research shows that valveless pumping may be explained on the basis of Newton's second law of motion by modeling a mass of fluid in the stiff segment driven by fluctuating pressure differences across its ends and pulling with it the entrained fluid in the compliant segment. The electrical analogy is that of a battery driving current in an electrical circuit through a load and also through the internal resistance of the battery. In a valveless pump the driving pressure difference is created by the reflection of pulse waves back and forth between the ends of the soft segment. These pulse waves are described by the classical wave equation and the Moens-Korteweg equation.

The pulse wave reflection hypothesis contains four essential assumptions:

(1) There are two segments connected in a loop, one of which is rigid and one of which is flexible

(2) Pressure waves are reflected without inversion between the ends of the flexible segment, creating a driving pressure across the ends of the stiff segment

(3) The velocity of the pressure waves is not constant, but varies with time

(4) The flexible segment acts like a battery that generates a certain mean pressure across its ends that can be used to drive flow through a "load", namely the stiff segment.

Variation in pulse wave velocity according to the Moens-Korteweg equation allows non-sinusoidal distortions to develop in the pressure waves, which are critical to generation of a mean pressure difference across the stiff segment. Non-linear elasticity of wall material is not needed to produce valveless pumping, because pulse wave velocity changes as a function of distension in a simple tube of constant elastic modulus, E.

The present analysis does not predict the details of fluid flow in flexible segment 1. However, since we consider an incompressible fluid, the average flow in any cross section of the loop of tubing should be the same after development of periodic steady state. Hence it is reasonable to choose the stiff part to show the existence of net flow. By using the "battery" metaphor, we avoid solving the hard problem of detailed flow in the soft segment, substituting the easier problem of flow in the stiff segment. This approach provides a relatively simple description of the physics of valveless pumps that permits calculation of several key values of interest, including instantaneous flow (averaged across the cross sectional area of the stiff segment) and time averaged mean flow in the stiff segment. These variables have been of most interest in previous discussions of valveless pumping[1, 2, 17]. As a result many heretofore unexplained and counterintuitive phenomena of at least one type of valveless pump can be understood on the basis of

Newton's second law of motion. These include the existence of nonzero average flow at certain frequencies, the existence of nonzero average flow in the opposite direction at other frequencies, the lack of substantial mean flow at some frequencies, the characteristic efficiency of valveless pumps, and flow reversal following abrupt change from one particular frequency to another.

VI. PROBLEMS AND EXERCISES

1. Suppose the relevant thicknesses h_1 and h_2 in Eq. (34) are the time averaged mean values during a compression cycle. Explain the small differences in calculated frequency peaks in Figure 7 for stroke volume = 0.25 ml versus stroke volume = 1.0 ml.

2. Using a slightly more general version of Eq. (35), predict shifts in peak frequency for valveless pumping if fluid density within the pump were changed from that of water (1.0 g/ml) to that of liquid mercury (13.6 g/ml).

3. Build a valveless pump as shown in Figure 2 from stiff laboratory tubing, such as clear Tygon®, and very thin, soft latex tubing such as a Penrose surgical drain. Include within the stiff segment a T-shaped filling port. Fill the system with water including a non-sticky marker material to visualize flow (shredded toilet paper works well). Place the pump on an overhead projector for classroom demonstration.

4. Predict behavior of a valveless pump such as that described in exercise (3). Weights, bent paperclips, a sample of the soft segment tubing, and a millimeter ruler are sufficient equipment. Cut a short ring shaped segment of tubing having axial width, a, about 0.5 cm. Let the tubing thickness be h, and the circumference be 2L, for flattened length, L. Study the elastic properties of the tubing by stretching the ring vertically between two bent paperclips, using a known weight, m, which exerts downward force mg. Proceed as follows. (a) First recall that Young's modulus E = stress/strain. Stress is force per unit area, and strain is fractional elongation $\Delta L/L$. Show algebraically that the numerator of the Moens-Korteweg equation is $Eh = \dfrac{mg}{2a(\Delta L/L)}$. (b) For weights producing about 20% strain, measure $\Delta L/L$ experimentally, and estimate Eh for the tubing material. The experimental value may be much larger than that for the standard model in Table 2 of this paper, since theoretical studies, including ours, have used very soft materials. (c) Now compute pulse wave velocity for the tube filled with water at low pressure using the Moens-Korteweg equation. (d) Using $f\lambda = s$, predict the locations of nodes and sweet spots, as shown in Figure 9, for compression of a valveless pump with a 100 cm long soft segment of such material. Nodes are compression points with zero net flow; sweet spots are compression points with maximal net flow. (e) Construct such a pump and compare predictions with experimental observations. Can you improve the experiment or the theory?

References

1. Liebau G. The principles of fluid flow in the heart. *Zeitschrift fuer Kreislaufforschung*. 1955;44:677-684
2. Jung E, Peskin CS. Two-dimensional simulations of valveless pumping using the immersed boundary method. *SIAM J. Sci. Comput.* 2001;23:19-45
3. Moser M, Huang J, Schwartz G, Kenner T, Noordergraaf A. Impedance defined flow, generalisation of william harvey's concept of the circulation--370 years later. *International journal of cardiovascular medicine and science*. 1998;1:205-211
4. Maron BJ, Hutchins GM. The development of the semilunar valves in the human heart. *American Journal of Pathology*. 1974;74:331-334
5. Halperin HR, Tsitlik JE, Beyar R, Chandra N, Guerci AD. Intrathoracic pressure fluctuations move blood during cpr: Comparison of hemodynamic data with predictions from a mathematical model. *Ann Biomed Eng*. 1987;15:385-403
6. Beattie C, Guerci AD, Hall T, Borkon AM, Baumgartner W, Stuart RS, Peters J, Halperin H, Robotham JL. Mechanisms of blood flow during pneumatic vest cardiopulmonary resuscitation. *J Appl Physiol*. 1991;70:454-465
7. Geddes LA, Baker LE. *Prinicples of applied biomedical instrumentation, second edition*. 1975.
8. Jung E. Eunok's home page. 2003;2003
9. Jung weogjih. Eunok's home page. 2002
10. Alderson H, Zamir M. Mechanical aspects of stenting on local hemodynamics. 2001;2001
11. Brophy JJ. *Basic electronics for scientists*. New York: McGraw-Hill; 1966.
12. Flaten JA, Parendo KA. Pendulum waves: A lesson in aliasing. *Am. J. Physics*. 2001;69:778-782
13. Remington J. Pressure-flow relations in the arterial system. In: Ray C, ed. *Medical engineering*. Chicago: Year Book Medical Publishers, Inc.; 1974:232-246.
14. Hueter TF, Bolt RH. *Sonics--techniques for the use of sound and ultrasound in engineering and science*. New York: John Wiley & Sons; 1955.
15. Schmid-Schonbein H. Hemorheology. In: Greger R, ed. *Comprehensive human physiology*. Berlin, Heidelberg: Springer-Verlag; 1996:1747-1792.
16. Posey J, Geddes L. Measurement of the modulus of elasticity of the arterial wall. *Cardiovascular Research Center Bulletin*. 1973;11:83-103
17. Jung E. Simulations of valveless pumping using the immersed boundary method. *Courant Institute of Mathematical Sciences*. 1999